

# Broken Strand Detection of Overhead Ground Wire by Image Processing and Morphological Feature Analysis

Shuangyong Zhou,<sup>1</sup> Houming Shen,<sup>2,3\*</sup> Jun Chen,<sup>1</sup>  
Jie Chen,<sup>1</sup> Linfeng Yu,<sup>1</sup> and Xianguo Li<sup>1</sup>

<sup>1</sup>State Grid Chongqing Ultra High Voltage Company, Chongqing 400039, China

<sup>2</sup>NARI GROUP Liability Corporation, State Grid Electric Power Research Institute Liability Corporation,  
Nanjing 211106, China

<sup>3</sup>Wuhan NARI Limited Liability Company, State Grid Electric Power Research Institute,  
Wuhan 430074, China

(Received June 16, 2023; accepted September 20, 2023)

**Keywords:** image processing, multithreshold, overhead ground wire, broken strand, morphological character, connection area

The inspection of overhead ground wires is an important guarantee to ensure the stable operation of the power system. The current method of the manual detection of broken strands of overhead ground wires is inefficient and prone to misjudgment. For this reason, a detection method of overhead ground wire broken strands by image processing and morphological feature analysis is proposed. First, the obtained image of the overhead ground wire is preprocessed to enhance the wire features. Subsequently, a complete effective binary image of the overhead ground line is obtained by combining the method of multithreshold segmentation and morphological processing based on the hue saturation value (HSV) color space. Finally, the morphological characteristics of the overhead ground connection area are analyzed, and the location of the broken strands is detected and marked by taking into account the difference between the broken strands and the normal ground. Furthermore, experimental analysis of overhead ground wires with complex backgrounds has confirmed that the method has high detection accuracy.

## 1. Introduction

High-voltage transmission lines play crucial roles in power systems, including transmission, regulation, and distribution. They serve as vital arteries of our country's power grid, ensuring its safe and stable operation.<sup>(1)</sup> The conductors of transmission lines are the essential carriers for electrical energy, and their stability and reliability directly impact the overall safety, stability, quality, and reliability of power supply by the system.<sup>(2)</sup> Traditional power line inspections have relied on manual methods, which require dedicated personnel and substantial human and material resources. However, this approach suffers from inefficiency and limitations. Therefore,

---

\*Corresponding author: e-mail: [shenhouming1993@163.com](mailto:shenhouming1993@163.com)  
<https://doi.org/10.18494/SAM4554>

it is imperative to study intelligent inspection and identification technologies to address these challenges effectively.<sup>(3)</sup>

European and American countries implemented the practical application of unmanned aerial vehicle (UAV) inspection systems for transmission lines early on,<sup>(4–6)</sup> enabling the automatic detection of anomalies in power lines. In recent years, China's power line inspection technology has kept pace with international standards, and the use of drones for distribution line inspections has become increasingly mature.<sup>(7,8)</sup> However, currently, even after obtaining images of transmission line conductors through inspections, manual observation is still required to detect conductor defects and obtain accurate results. This approach not only has low efficiency but is also susceptible to subjective factors, leading to less precise detection.<sup>(9,10)</sup> To improve the detection efficiency, an embedded automatic fault detection algorithm based on image processing has been designed.<sup>(11–13)</sup> A method for detecting conductor fractures and surface defects in transmission lines using UAVs has also been proposed.<sup>(14)</sup> This method can be used to monitor the health condition of the conductors and ensure the normal operation of the transmission lines. To achieve the high-precision detection of obscured insulators in transmission lines, You-only-look-once (YOLO) was employed for insulator recognition and localization, enabling real-time detection of high-voltage line insulators.<sup>(15)</sup> In Ref. 16, a deep-learning-based method was proposed for detecting insulator faults in aerial images of high-voltage transmission lines. This method is specifically designed to detect insulator faults in aerial images with complex backgrounds. By incorporating feature pyramid networks and an improved loss function into the cross stage partial dense (CSPD)-YOLO model, the accuracy of insulator fault detection is enhanced. Reference 17 describes the implementation of a fault detection system for conductor fractures in transmission lines using grayscale variance normalization and average intensity methods in OpenCV and Python. In ref. 18, Li *et al.* reported the first use of UAVs to capture images of transmission lines. Then, on the basis of the FCN network, image segmentation was performed on the captured images to extract the transmission line information. Subsequently, the specific image features of conductor fractures were utilized to extract the image features of each sliding window along the axis of the transmission line. This process allows for the identification of windows containing abnormal feature parameters, enabling the precise detection and localization of conductor fractures in transmission lines.

However, in the aforementioned literature, the complexity of the background in aerial ground wire images caused by the shooting angle was not fully considered when detecting the broken strands of transmission line conductors. Aerial ground wire images often contain low-resolution backgrounds such as trees, houses, and roads, which can pose challenges in identifying broken wire strands and easily lead to false detections or missed detections. To address this problem, in this paper, we propose an aerial ground wire broken strand detection method based on image processing and morphological feature analysis. Firstly, the acquired aerial ground wire images are preprocessed to enhance the wire features. Then, by combining a multithreshold segmentation based on the hue saturation value (HSV) color space and morphological processing methods, a binary image of the complete and effective aerial ground wire is obtained. Finally, morphological feature analysis is performed on the connected regions of the aerial ground wire, taking into consideration the distinguishing features of the broken strand regions and the normal

wire, thus detecting the locations of the broken strands and annotating them. Through experimental analysis, the proposed method can overcome the challenges posed by complex backgrounds, thereby improving the accuracy and robustness of broken strand detection.

## 2. Overhead Ground Wire Image Preprocessing

Because of limitations in the shooting scenes and environments, the acquired overhead line images exhibit complex backgrounds and significant noise and speckle interference, which adversely affect the segmentation of the ground line regions and the subsequent detection of fracture positions. To enhance the accuracy of fracture position detection, it is necessary to preprocess the original images to reduce noise interference, thereby improving the stability and accuracy of subsequent processing. Common preprocessing measures include image denoising, image enhancement, and color model conversion.

### 2.1 Image denoising

The effect of image capture devices or the surrounding environment may have a negative impact on image quality, resulting in the presence of noise in the images. These noise signals degrade the quality of the images and may confound useful information, thereby reducing the stability and accuracy of image processing. To reduce noise interference during the image processing, we employ mean filtering. The principle of mean filtering involves averaging the pixel values within a neighborhood region of each pixel in the image to obtain a new pixel value. The formula for mean filtering is

$$I_{smooth}(x, y) = \frac{1}{(2r+1)^2} \sum_{i=-r}^r \sum_{j=-r}^r I(x+i, y+j), \quad (1)$$

where  $I_{smooth}(x, y)$  represents the filtered pixel value in the image,  $(x, y)$  represents the coordinates of the pixel point to be subjected to the smoothing filter,  $I(x+i, y+j)$  represents the pixel values within the neighborhood centered at  $(x+i, y+j)$ , and  $r$  represents the radius of the filter.

### 2.2 Threshold segmentation

Image segmentation is a crucial step in image processing and also one of the most critical tasks. Image segmentation refers to the process of dividing the pixels in an image into several distinct sets, with each set representing an entity or background in the image. Thresholding is a common method used to convert grayscale images into binary images on the basis of the relationship between pixel values and a specified threshold.<sup>(19)</sup> Essentially, it involves transforming the input image  $f$  into the output image  $g$ , in accordance with the following transformation formula:

$$g(i, j) = \begin{cases} 1, & f(i, j) \geq T \\ 0, & f(i, j) < T \end{cases} \quad (2)$$

where  $T$  represents the threshold value. For elements in the target region,  $g(i, j) = 1$  takes on a certain value,  $g(i, j) = 1$ , whereas for elements in the background,  $g(i, j) = 0$  is assigned.

### 2.3 Overhead wire region extraction

Effective and accurate segmentation of ground wire regions is crucial for detecting fracture positions, and precise segmentation methods are an important focus in the current field of object detection. In this study, the challenge in extracting ground wire regions lies in addressing the color discrimination issue as overhead wires have a very similar color to insulators, making it difficult to differentiate between the two by conventional methods. Moreover, overhead wire images often contain sky and forest backgrounds, resulting in rich background colors and considerable noise interference, which pose significant difficulties in accurately extracting the ground wire regions. Referring to previous research, in this work, we build upon threshold segmentation and employ a multithreshold segmentation method based on the HSV color space<sup>(20,21)</sup> to segment candidate target regions. Then, the morphological characteristics of the connected components are analyzed to extract the ground wire regions. This method effectively addresses the issue of background noise interference with overhead wires and separates them from the insulator regions, providing a prerequisite for detecting fracture positions in subsequent steps.

#### 2.3.1 Multithreshold segmentation based on HSV color space

The HSV color space consists of three components: hue, saturation, and value. The hue component represents the color category, saturation represents the purity of the color, and value represents the brightness or darkness of the color. This color space provides a better representation of prominent color features, and it is widely utilized in the field of image processing. In the conversion from the RGB color space to the HSV color space, the three components of HSV are as follows:

$$H = \begin{cases} 0^\circ, & \text{if } \max = \min \\ 60^\circ \times \frac{G - B}{\max - \min} + 0^\circ, & \text{if } \max = R \text{ and } G \geq B \\ 60^\circ \times \frac{G - B}{\max - \min} + 360^\circ, & \text{if } \max = R \text{ and } G < B \\ 60^\circ \times \frac{B - R}{\max - \min} + 120^\circ, & \text{if } \max = G \\ 60^\circ \times \frac{R - G}{\max - \min} + 240^\circ, & \text{if } \max = B \end{cases} \quad (3)$$

$$S = \begin{cases} 0, & \text{if } \max = 0 \\ \frac{\max - \min}{\max}, & \text{if } \max \neq 0 \end{cases} \quad (4)$$

$$V = \max. \quad (5)$$

Here,  $R$ ,  $G$ , and  $B$  represent the values of the red, green, and blue color channels, respectively. “ $\max$ ” refers to the maximum value among  $R$ ,  $G$ , and  $B$ , while “ $\min$ ” refers to the minimum value among  $R$ ,  $G$ , and  $B$ .

Threshold segmentation is one of the most commonly used methods of image segmentation, where pixels in an image are classified into different categories on the basis of their grayscale values and predetermined threshold values. In the process of overhead power wire area segmentation, conventional single-threshold segmentation methods are hindered by the interference of background noise from the sky and dense forests, making it challenging to accurately extract the overhead power wire regions from complex scenes. To address this issue, we propose a multithreshold segmentation method by defining a threshold range to divide the pixels into distinct regions, followed by the application of morphological operations to extract the overhead power wire areas.

The multithreshold segmentation algorithm based on the HSV color space is a method that utilizes the hue component to segment the image. The specific steps are as follows.

- (1) Convert the image from the RGB color space to the HSV color space.
- (2) Select an appropriate number of thresholds and determine the range for each threshold based on the specific application scenario.
- (3) Perform multithreshold segmentation on the hue component of the HSV color space, dividing the image into several regions.
- (4) Calculate the average color value of pixels within each region and merge regions with similar color values into a cohesive entity.
- (5) Further process the image using methods such as morphological operations to eliminate noise and unnecessary regions.

### 2.3.2 Morphological processing-based extraction of ground wire regions.

By the multithreshold segmentation method, multiple connected regions can be obtained, including conductor regions, insulator regions, overhead ground wire regions, and various small interfering areas. Firstly, denoising and closing operations<sup>(22)</sup> are performed on the segmented image to eliminate small noise interference and form large connected regions of interest. Then, calculations are performed on all connected regions to filter and extract the overhead ground wire regions. The formula for calculating the area of a connected region is

$$A = \sum_{i=1}^n \sum_{j=1}^m I(i, j), \quad (6)$$

where  $A$  represents the area of the connected region,  $I(i, j)$  represents the value  $(i, j)$  of a pixel point, and  $n$  and  $m$  represent the width and height of the image, respectively.

The principle of this formula is to sum up the values of all pixels within the connected region, resulting in the area of the connected region. In this study, by analyzing the overhead ground wire images, it was found that the overhead ground wire occupies the largest area, and corresponds to the largest connected region in terms of area. By sorting and selecting the largest connected region, the overhead ground wire region can be extracted.

## 2.4 Morphological processing

Morphological processing is an image processing technique that is primarily used for processing and analyzing the shapes and structures in an image.<sup>(23)</sup> Its main purpose is to change or enhance features such as shape, size, and orientation in an image to achieve operations such as segmentation, noise reduction, and feature extraction. Common morphological processing methods include dilation, erosion, open operation, closed operation, gradient operation, top-hat operation, and bottom-hat operation.

## 3. Differential Feature Analysis

### 3.1 Analysis of broken strand regions

Through the analysis of collected aerial wire images containing broken strands, the following characteristics of broken strand regions are typically observed.

- (1) When the outer surface of the aerial wire is fractured, broken strands exhibit the convergence of several fine wires with different slopes.
- (2) Typically, the broken strands will appear as tiny branches that are limited in length and do not span the entire image.
- (3) The pixel gradient and the rotational gradient angle of pixel blocks at the site of broken strands undergo changes.

A model of broken strands in overhead ground wires, based on the characteristics of broken strands in overhead ground wires, is illustrated in Fig. 1.

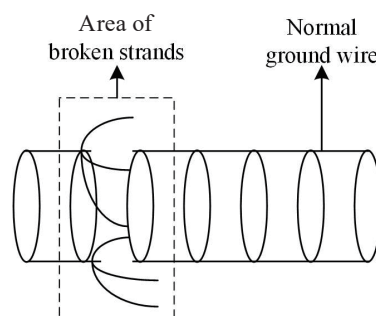


Fig. 1. Broken strand model of overhead ground wire.

### 3.2 Image gradient and direction

The image gradient refers to the rate of change of a pixel in both the  $x$  and  $y$  directions (relative to neighboring pixels). It is a two-dimensional vector composed of two components: the change in the  $x$ -axis and the change in the  $y$ -axis. By calculating these two components, a two-dimensional vector representing the image gradient of that pixel is obtained. Taking the arctan of the vector yields the gradient angle. The gradient of the image function  $f(x, y)$  at point  $(x, y)$  is a vector with magnitude and direction. It can be represented as  $G_x$  and  $G_y$ , which respectively indicate the gradients in the  $x$  and  $y$  directions. This gradient vector can be expressed as below.

$$\nabla f(x, y) = [G_x, G_y]^T = \left[ \frac{\partial f}{\partial x}, \frac{\partial f}{\partial y} \right]^T \quad (7)$$

The magnitude of this vector is given by

$$\text{mag}(\nabla f) = g(x, y) = \sqrt{\frac{\partial^2 f}{\partial x^2} + \frac{\partial^2 f}{\partial y^2}}. \quad (8)$$

The direction angle is

$$\phi(x, y) = \arctan \left| \frac{\frac{\partial f}{\partial y}}{\frac{\partial f}{\partial x}} \right|. \quad (9)$$

The direction of the gradient is the direction in which the function  $f(x, y)$  changes most rapidly. Gradient values will be larger at edges in an image. Conversely, when there are relatively smooth regions in the image with small changes in grayscale values, the corresponding gradients will also be smaller.

### 3.3 Detection of broken strands in overhead ground wires

As revealed by the analysis above, there are obvious feature differences between broken strands and normal ground wires. The detection of broken strands based on the gradient changes of the broken strand pixels and the rotation gradient angles of the image blocks can be achieved by the following steps.

- (1) Image preprocessing: binary and smoothing processing is applied to the extracted overhead ground wires to reduce noise interference.
- (2) Broken strand detection: the binary image of the overhead ground wire pixels is scanned to calculate the number of adjacent pixel transitions  $S$  using

$$S = \sum_{j=1}^{2h} |D(j)|, \quad (10)$$

$$\begin{cases} D(j) = 1, f(j) \neq f(j+1) \\ D(j) = 0, f(j) = f(j+1) \end{cases}, \quad (11)$$

where  $D(j) = f(j) - f(j-1)$ , ( $j = 1, 2, 3, \dots, 2h$ ),  $f(j)$  means scan column, ( $j = 1, 2, 3, \dots, 2h$ ).

(3) Broken strand identification: For each pixel block, the gradient angles of its internal pixels are computed. The presence of a broken strand is determined on the basis of the variations in the width of the power wire trajectory. The calculation formula is as follows.

$$k_j = \frac{d_j - d_{j+1}}{r/2} = \frac{2 * (d_j - d_{j+1})}{r} \quad (12)$$

(4) Broken strand localization: From the calculations performed in steps (2) and (3), the positions of broken strands are detected and annotated. The detection formula is as follows.

$$\begin{cases} \text{Broken strand occurrence, } k_j > 1 \cap S > 2 \\ \text{No broken strand occurrence, } 0 \leq k_j \leq 1 \cap S = 2 \end{cases} \quad (13)$$

#### 4. Detection of Broken Strands in Overhead Ground Wires by Image Processing and Morphological Feature Analysis

The specific process for detecting broken strands in overhead ground wires based on image processing and morphological feature analysis includes the following steps and is illustrated in Fig. 2.

Step 1: Images of overhead ground wires containing broken strands are collected.

Step 2: Preprocessing is performed on the collected images.

Step 3: A multithreshold segmentation method based on the HSV color space is utilized to obtain connected regions containing the overhead ground wires.

Step 4: Connected regions corresponding to the overhead ground wires are selected from the candidate regions using morphological processing methods.

Step 5: The characteristic differences between the regions with broken strands and the normal sections of the overhead ground wires are analyzed. An algorithm is designed to detect and mark the locations of broken strands.

Step 6: The binary image of the overhead ground wires is scanned to determine the presence of broken strand regions. If broken strand regions exist, the process proceeds to the next step. If there are no broken strand regions, the process terminates directly.

Step 7: The positions of the broken strand regions within the overhead ground wire region are identified using Eq. (12).



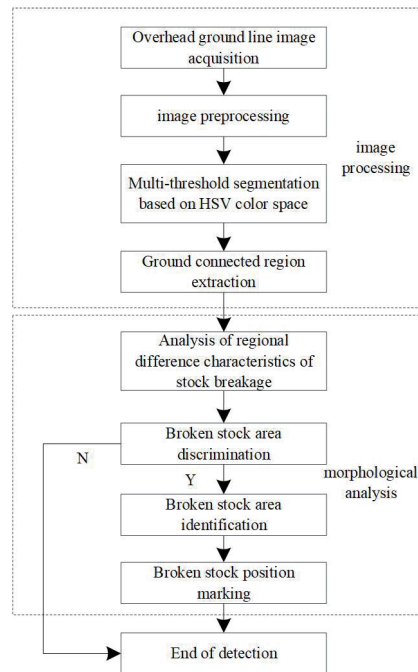


Fig. 2. Detection process of broken strands of overhead ground wire.

Step 8: The locations of the broken strand regions are marked using rectangular bounding boxes and annotated as “broken strand”.

Step 9: Detection process concludes.

## 5. Experimental Testing and Analysis of Results

To validate the effectiveness and accuracy of the proposed algorithm in the extraction of overhead ground wires and detection of broken strand locations, we conducted separate investigations for wire extraction and broken strand detection. For the extraction of overhead ground wires, a variety of images depicting overhead ground wires from different scenes were selected for experimentation. A comparison was made with several commonly used segmentation algorithms to verify the effectiveness of the proposed method. Additionally, we performed experiments on images containing broken strands of overhead ground wires and provided specific implementation cases to evaluate the accuracy of the algorithm in detecting broken strand locations.

### 5.1 Comparison of different segmentation methods

To validate the effectiveness of the proposed method for extracting overhead ground wire regions, the proposed method and several mainstream traditional segmentation methods were compared. The corresponding results are shown in Figs. 3 to 7. The results indicate that threshold

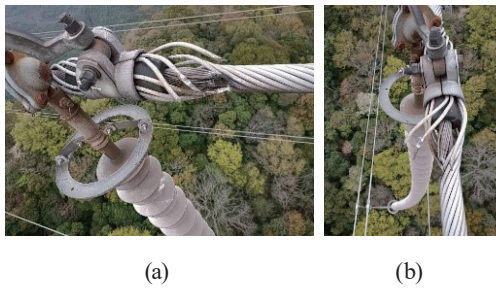


Fig. 3. (Color online) Overhead ground wire inspection image.

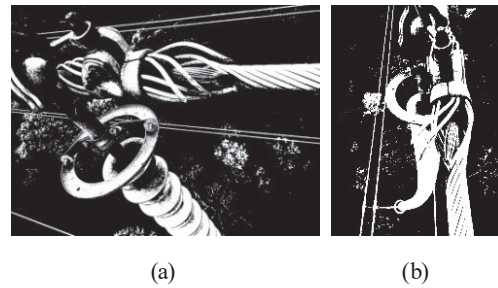


Fig. 4. Threshold segmentation.

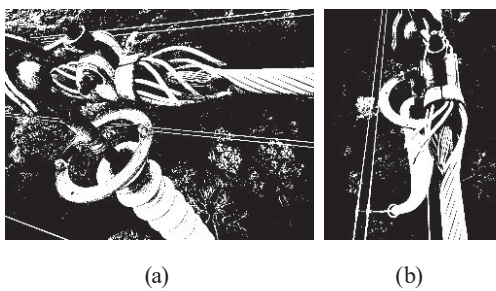


Fig. 5. *K*-means clustering segmentation.

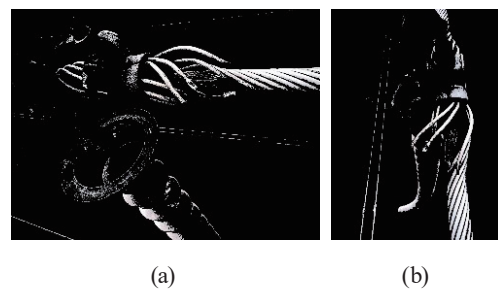


Fig. 6. Multithreshold segmentation.

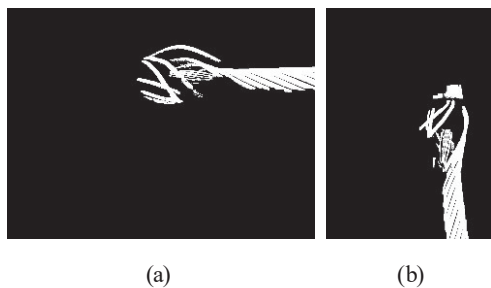


Fig. 7. Method proposed in this article.

segmentation<sup>(24)</sup> and *K*-means clustering segmentation<sup>(25)</sup> methods can segment the overhead ground wire regions, but they are highly susceptible to background interference and cannot differentiate between overhead ground wires and insulators. The multithreshold segmentation method based on the HSV color space can effectively distinguish between overhead ground wires and insulators with minimal interference from the background. In this study, on the basis of the multithreshold segmentation method using the HSV color space, morphological operations are applied to the segmented connected regions, resulting in the ideal extraction of overhead ground wire regions.

## 5.2 Analysis of detection results of broken strands

The original overhead ground wire captured in this experiment is shown in Figs. 8(a) and 8(b). Both images depict the same overhead ground wire captured from different angles and include the overhead ground wire, insulators, support structures, conductors, and a forest background; the overhead ground wire and insulator regions appear as light gray in color. The resolution is  $1706 \times 1279$  pixels with horizontal and vertical resolutions of 96 dpi for the image in Fig. 8(a) and  $618 \times 825$  pixels and 96 dpi, respectively, for the image in Fig. 8(b). In both images, there is only one area with a broken strand where the conductor splits and converges into several small branches. Figures 9(a) and 9(b) display the results of the proposed method. It can be observed that the proposed method effectively separates and extracts the overhead ground wire region from the background, significantly improving the efficiency of subsequent broken strand location detection. Figures 10(a) and 10(b) present the annotated results of broken strand locations. By analyzing the differential morphological features between the broken strand area and the normal overhead ground wire region, the broken strand area is detected on the basis of the variations in pixel gradients and the rotational gradient angles of pixel blocks. The detected broken strand areas are then annotated in the original images.

Table 1 lists more results of broken strand overhead ground wire inspection. As can be seen from Table 1, the broken strand portion of the overhead ground wire can be successfully detected by the proposed method.

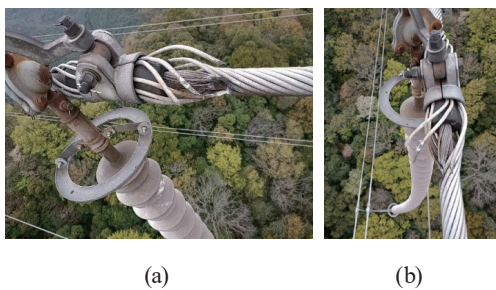


Fig. 8. (Color online) Overhead ground wire inspection image.

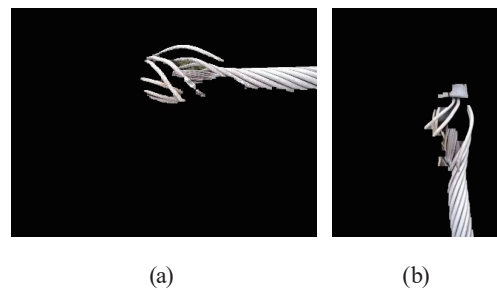


Fig. 9. Ground wire area extraction.

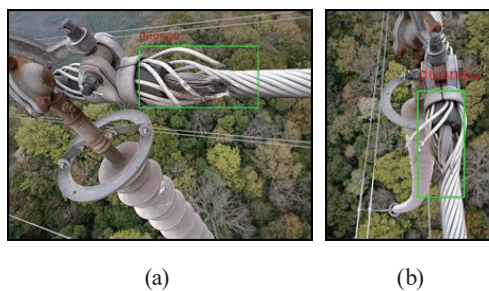


Fig. 10. (Color online) Ground wire area marking..


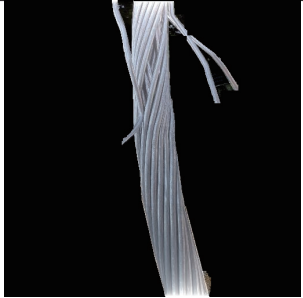


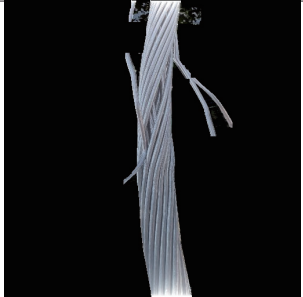

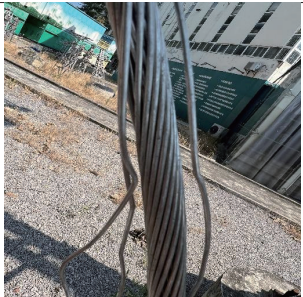



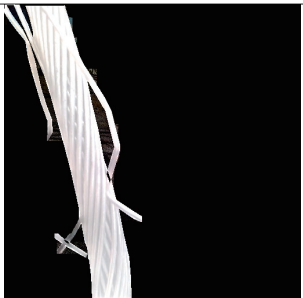

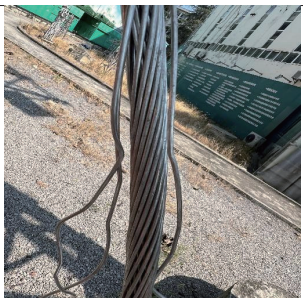

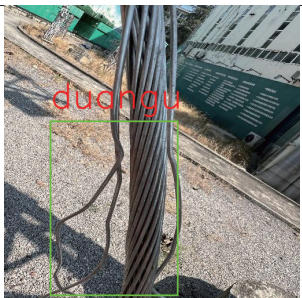


Table 1  
(Color online) Results of broken strand overhead ground wire inspection.

Overhead ground wire inspection image	Ground wire area extraction	Ground wire area marking	Correct detection
			Yes
			Yes
			Yes
			Yes
			Yes



Table 1  
 (continued) (Color online) Results of broken strand overhead ground wire inspection.

Overhead ground wire inspection image	Ground wire area extraction	Ground wire area marking	Correct detection
			Yes
			Yes
			Yes
			Yes
			Yes

## 6. Conclusions

The traditional method of manual inspection can no longer meet the needs resulting from the rapid advancement of the power transmission network. The intelligent inspection of overhead ground wires represents the future trend. In this article, we proposed an aerial power wire image broken strand detection method based on image processing and morphological feature analysis. It effectively extracted the overhead ground wire region and, on the basis of the differential characteristics between the broken strand and normal sections, utilized the pixel block rotational gradient angle variation ratio to diagnose the broken strand location and then annotated it with a rectangular box. Experimental results demonstrated that the proposed method can accurately diagnose broken strand locations in complex backgrounds, exhibiting excellent precision and applicability. By integrating this method with diagnostic equipment, it can effectively address the issue of human error in the manual inspection of overhead ground wires and provide technical support for their maintenance and repair. In the future, we will try to effectively embed deep learning networks into this detection model to better respond to the contextually more complex broken-strand detection problems, which may exist in engineering practice.

## References

- 1 Y. W. Yang, H. J. Hou, and Y. Yang: Power Syst. Technol. **41** (2017) 3648. <https://doi.org/10.13335/j.1000-3673.pst.2017.0094>
- 2 X. Huang, X. Zhang, Y. Zhang, L. Yang, C. Liu, and W. Li: Autom. Electr. Power Syst. **44** (2020) 201. <https://doi.org/10.7500/AEPS20190122004>
- 3 X. Peng, L. Yi, and J. Qian: High Voltage Eng. **46** (2020) 384. <https://doi.org/10.13336/j.1003-6520.hve.20200131002>
- 4 A. Pagnano, M. Höpf, and R. Teti: Procedia Cirp **12** (2013) 234. <https://doi.org/10.1016/j.procir.2013.09.041>
- 5 C. Martinez, C. Sampedro, A. Chauhan, J. François Collumeau, and P. Campoy: Eng. Appl. Artif. Intell. **71** (2018) 293. <https://doi.org/10.1016/j.engappai.2018.02.008>
- 6 W. L. Fu, X. Jiang, B. L. Li, C. Tan, B. Chen, and X. Chen: Meas. Sci. Technol. **34** (2023) 045005. <https://doi.org/10.1088/1361-6501/acabdb>
- 7 Q. P. Lai, J. Yang, B. D. Tan, L. Wang, S. Y. Fu, and L. W. Han: Electr. Power **52**(2019) 31. <https://doi.org/10.11930/j.issn.1004-9649.201806102>
- 8 W. Y. Sha, N. H. He, P. Ding, and S. Chen: Electr. Meas. Instrum. **59** (2022) 158. <https://doi.org/10.19753/j.issn1001-1390.2022.05.021>
- 9 W. Li, L. L. Tang, and H. H. Wu: Remote Sens. Technol. Appl. **34** (2019) 269. <https://doi.org/10.11873/j.issn.1004-0323.2019.2.0269>
- 10 B. Li and C. Chen: Electr. Power **52** (2019) 82. <https://doi.org/10.11930/j.issn.1004-9649.201805203>
- 11 S. S. Han, H. Ru, and J. Lee: IEEE Trans. Power Delivery **24** (2009) 2319. <https://doi.org/10.1109/TPWRD.2009.2028534>
- 12 X. Jiang: Automat. Electr. Power Syst. **35** (2011) 78. <https://doi.org/dlxt.0.2011-15-016>
- 13 S. Fang, L. Sheng, and X. Y. Wang: 2020 IEEE 4th Information Technology, Networking, Electronic and Automation Control Conf. (ITNEC) (IEEE, 2020) 1715. <https://doi.org/10.1109/ITNEC48623.2020.9084907>
- 14 Y. Zhang, X. Huang, J. Jia, and X. Liu: IEEE Access **7** (2019) 59022. <https://doi.org/10.1109/ACCESS.2019.2914766>
- 15 D. Sadykova, D. Pernebayeva, M. Bagheri, and A. James: IEEE Trans. Power Delivery **35** (2019) 1599. <https://doi.org/10.1109/TPWRD.2019.2944741>
- 16 C. Liu, Y. Wu, J. Liu, and H. Xu: Appl. Sci. **11** (2021) 4647. <https://doi.org/10.3390/app11104647>
- 17 P. G. Shivani, S. Harshit, C. V. Varma, and R. Mahalakshmi: 2020 4th Int. Conf. Electronics, Communication and Aerospace Technology (ICECA). (IEEE, 2020) 1016. <https://doi.org/10.1109/ICECA49313.2020.9297639>
- 18 F. W. Li, Y. Z. Yu, L. F. Yuan, X. Chao, and J. Y. Chen: J. Geomatics **46** (2021) 132. <https://doi.org/10.14188/j.2095-6045.2020579>

- 19 Z. H. Yuan, W. L. Fu, B. L. Li, and B. Wen: Power Syst. Prot. Control **50** (2022) 98. <https://doi.org/10.19783/j.cnki.pspc.210355>.
- 20 P. Hao and L. Fang: Comput. Sci. **47** (2020) 220. <https://doi.org/10.11896/jsjcx.191000180>
- 21 Y. F. Xia: Comput. Eng. Software **41** (2020) 170. <https://doi.org/10.3969/j.issn.1003-6970.2020.07.034>
- 22 S. Liu, H. Liu, T. S. Bi, X. J. Yang, and J. Yang: Power Syst. Technol. **1** (2023) 12. <http://kns.cnki.net/kcms/detail/11.2410.tm.20221026.1432.005.html>
- 23 S. H. Wang, L. L. Niu, H. Li, and W. T. Huang: High Voltage Appar. **55** (2019) 201. <https://doi.org/10.13296/j.1001-1609.hva.2019.02.029>
- 24 W. L. Fu, J. W. Tan, X. H. Wu, T. Chen, and H. Wenbin: Electr. Power Autom. Equip. **39** (2019) 203. <https://doi.org/10.16081/j.issn.1006-6047.2019.07.030>
- 25 L. Chen, J. W. Sun, L. Y. Wang, H. Z. Z., and Q. G. Sun: Power Syst. Technol. **44** (2020) 2343. <https://doi.org/10.13335/j.1000-3673.pst.2019.2052>

## About the Authors

**Shuangyong Zhou** works in the ultrahigh voltage branch of the State Grid Chongqing Electric Power Company as the head of the southeast branch of Chongqing and has been engaged in the inspection of transmission lines. (shenhouming1993@163.com)

**Houming Shen** received his B.S. and M.S. degrees from Qingdao University. Since 2018, he has been working as an engineer in Wuhan Nanrui Co., Ltd. of the State Grid Electric Power Research Institute. His main research direction is intelligent operation and maintenance of power transmission and transformation equipment. (shenhouming@sgepri.sgcc.com.cn)

**Jie Chen** received his B.S. degree from Guangzhou University and his M.S. degree from Shanghai Electric Power University. Since 2016, he has been working in the State Grid Chongqing EHV Company, and his main research directions are electric power big data and intelligent operation and inspection of transmission lines. (chenjie@cq.sgcc.com.cn)

**Linfeng Yu** received his B.S. degree from Southwest Jiaotong University and his M.S. degree from Chongqing University. From 2014 to the present, he has been working in the State Grid Chongqing EHV Company. His main research directions are intelligent inspection of overhead transmission lines, live maintenance, and intelligent applications. (yulinfeng@cq.sgcc.com.cn)